ELSEVIER

Chemical Geology 153 (1999) 241–248

CHEMICAL GEOLOGY
INCLUDING
ISOTOPE GEOSCIENCE

High-resolution $\delta^{18}O$ analysis of tooth enamel phosphate by isotope ratio monitoring gas chromatography mass spectrometry and ultraviolet laser fluorination

Alison M. Jones [a,*], Paola Iacumin [b], Edward D. Young [a]

[a] *Department of Earth Sciences, University of Oxford, Parks Road, Oxford, OX1 3PR, UK*
[b] *Università degli Studi di Trieste, Dipartimento di Scienze Geologiche, Ambientali e Marine, Via E. Weiss, 6, 34100 Trieste, Italy*

Received 10 February 1998; accepted 11 September 1998

Abstract

The viability of oxygen isotope analysis of tooth enamel by UV laser ablation and fluorination has been demonstrated by comparison with the Ag_3PO_4 extraction method. In-situ analyses by UV laser fluorination using both isotope ratio mass spectrometry and isotope ratio monitoring gas chromatography mass spectrometry (irm-GCMS) microanalysis are comparable to those of the Ag_3PO_4 method with a mean precision of $\pm 0.4‰$ (1σ) for samples with $\delta^{18}O$ values ranging from 10.8 to 20.8‰. UV laser ablation provides spatial resolution of 100 μm or less with no laser reaction rim. These data show that irm-GCMS offers a combination of spatial and analytical precision for in-situ sampling of biogenic apatites previously unobtainable by other means.

Keywords: Oxygen isotopes; UV laser; Microanalysis; Teeth

1. Introduction

The oxygen isotope composition of skeletal material has been widely used in palaeoclimatic research (Longinelli, 1984; Luz and Kolodny, 1985; Ayliffe and Chivas, 1990; D'Angela and Longinelli, 1990; Ayliffe et al., 1994; Fricke and O'Neil, 1996; Iacumin et al., 1996) because of its sensitivity to changing climatic conditions. Recent studies (e.g., Ayliffe et al., 1994) suggest that because tooth enamel has lesser amounts of organic material and larger crystals than bone, cementum or dentine, it is less prone to degradation and recrystallisation. Enamel is most likely to retain an original isotopic signal for longer periods and is thus favoured for palaeoclimatic research. The traditional methods of apatite oxygen extraction can be lengthy and complicated and only recently have laser-based methods (Kohn et al., 1996; Sharp and Cerling, 1996) been devised to enhance the rapidity and spatial resolution of bulk hydroxylapatite $^{18}O/^{16}O$ analysis.

Biogenic apatite can be represented by the formula $Ca_5(PO_4)_{3-x}(CO_3)_xOH_{1-y}F_y$ where x and y are typically near 0.3 and 0.5, respectively (e.g., McConnell, 1973), and as much as 10% of total oxygen derives from CO_3^{2-} that replaces PO_4^{3-} in biogenic apatite. Traditionally, the extraction of PO_4^{3-} groups from biogenic apatite for oxygen isotope analysis involves a long and tedious process

* Corresponding author.

0009-2541/99/$ - see front matter
PII: S0009-2541(98)00162-4

whereby approximately 10–40 mg of phosphate sample is acidified, reprecipitated as Ag or Bi phosphate and then reduced at high temperature with fluorinating compounds (Kolodny et al., 1983; Luz et al., 1984; Wright and Hoering, 1989), Br_2 (Stuart-Williams et al., 1995), or graphite (O'Neil et al., 1994) to produce CO_2 or O_2 gas. These methods have typical analytical reproducibilities of ± 0.1–0.3‰ (1σ) but are destructive to a large part of the sample and do not allow for resolution of spatial variations in $^{18}O/^{16}O$, except in cases where teeth are large and enamel is abundant (e.g., Fricke and O'Neil, 1996).

Precipitation as Ag_3PO_4 or $BiPO_4$ ensures that oxygen from the PO_4^{3-} group alone is analysed. Laser-based methods (Kohn et al., 1996; Cerling and Sharp, 1996; this study), where the sample is analysed in bulk, necessarily extract oxygen from both PO_4^{3-} groups and other oxygen-bearing groups within the hydroxylapatite structure. Iacumin et al. (1996) have shown that CO_3^{2-} is enriched in ^{18}O relative to PO_4^{3-} by an average 9.2‰ in pristine hydroxylapatites, i.e., $\Delta_{CO_3-PO_4} = 9.2$‰. It is likely, therefore, that the CO_3^{2-} group will contribute approximately 0.5–0.9‰ to the $\delta^{18}O$ value of a bulk carbonate hydroxylapatite analysis. Thus bulk oxygen laser extraction is expected to yield $\delta^{18}O$ values higher than the Ag_3PO_4 method unless oxygen from the hydroxyl site has sufficiently low $^{18}O/^{16}O$ to balance the carbonate contribution. The value of Δ_{OH-PO_4} in carbonate hydroxylapatite has not been determined.

In this communication we demonstrate the viability of using UV laser fluorination combined with irm-GCMS for precision $^{18}O/^{16}O$ analysis of biogenic apatite with high spatial resolution as an alternative to conventional chemical extraction procedures. UV laser fluorination offers several advantages over previously published infrared laser methods, including elimination of the problem of incomplete oxygen extraction and the need for data correction factors.

2. Infrared laser fluorination of phosphate

Infrared (IR) laser-based methods for biogenic apatite $^{18}O/^{16}O$ determinations exhibit offsets from Ag_3PO_4 precipitation methods that cannot be easily explained by the presence of carbonate and hydroxyl oxygen. For example, IR laser fluorination of powdered phosphates (Kohn et al., 1996) has proved successful in reducing the amount of sample required for $^{18}O/^{16}O$ determination in biogenic phosphate from tens of mg to approximately 0.5 to 2 mg. However, analytical yields using this method are approximately 80% and all data require a correction, usually of $+1.7$‰ based on comparisons with analyses of inorganic fluorapatites (which are carbonate and hydroxyl free) by conventional fluorination in Ni reaction vessels (Kohn et al., 1996).

In a largely unpublished study, Young (1993) explored the efficacy of IR laser heating in fluorine for quantitative extraction of oxygen from phosphate minerals using micro-Raman and infrared spectroscopy of both solid and gaseous reaction products. Experiments showed that oxygen can be lost from

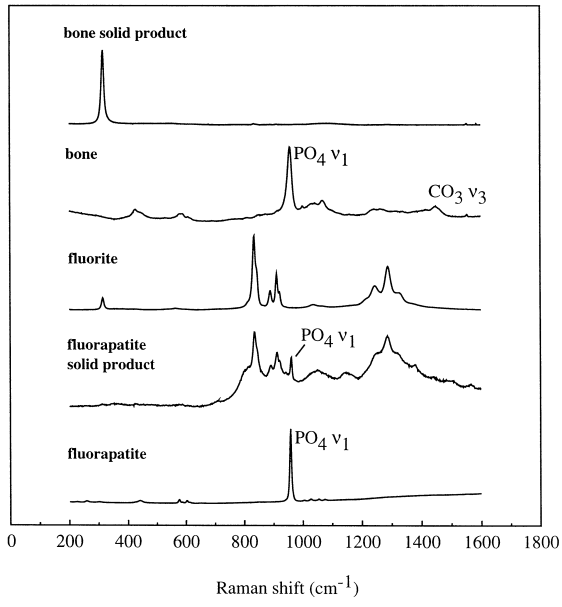

Fig. 1. Micro-Raman spectra of fluorapatite, bone, and solids remaining after infrared fluorination of these materials. Also shown is a spectrum for fluorite for reference. Fluorite has a single significant band at 319 cm^{-1} resulting from fluorine–fluorine (F–F) oscillations. The additional broad bands from approximately 800 to 1400 wavenumbers are extraneous, resulting from fluorescence. Similar fluorescence is exhibited by the fluorapatite solid product. Bone carbonate hydroxylapatite is seen to react completely to fluorite while fluorapatite is incompletely reacted. Note the sharp orthophosphate band at 980 cm^{-1} and the absence of the F–F peak diagnostic of fluorite in the fluorapatite product.

the analyte gas to both gaseous and solid products. Analyses were carried out on cryptocrystalline carbonate hydroxylapatite (bone) and showed that this mineral readily reacts with F_2, when heated by IR laser, to form pure CaF_2 as the sole solid product (Fig. 1); no orthophosphate (PO_4^{3-}) could be detected within the solid. However, under identical conditions, single crystals of fluorapatite were not uniformly converted to pure solid CaF_2 despite prolonged laser heating. Instead PO_4^{3-} was detected within the remaining solid (Fig. 1). Infrared spectra of gaseous products from these experiments also revealed the presence of several oxygen-bearing species, including POF_3 and other unidentified phosphoryl halide compounds (Fig. 2).

The low yields and systematic $\delta^{18}O$ offset noted in enamel and bone analyses (e.g., Kohn et al., 1996) are thus likely to be the result of the formation of gaseous ^{18}O enriched P–O–F_x compounds and, in the case of fluorapatite, the incomplete breakdown of orthophosphate. As fluorapatite is more resistant to fluorination during laser heating, extrapolation of correction factors to carbonate hydroxylapatite may be suspect.

A different sort of infrared laser-based phosphate oxygen extraction technique is described by Cerling and Sharp (1996). In this procedure the sample is directly heated by IR laser in flowing helium gas, with no fluorinating reagent, to produce a small amount of CO_2 gas. The carbon is derived from the structural carbonate but the sources of oxygen are unclear. Comparison of $\delta^{18}O$ values obtained using this method with those of other methods show inconsistent variations of up to 2.9‰ with an average offset of 1.2‰. Cerling and Sharp (1996) attribute this offset to high $^{18}O/^{16}O$ from the carbonate group or from actual intra-tooth variations. The probable offset of high $^{18}O/^{16}O$ carbonate by low $^{18}O/^{16}O$ hydroxyl was not addressed.

Spot sizes as small as 200 μm can be analysed using IR laser heating methods (Cerling and Sharp, 1996). Practical spatial resolution, however, is dictated by the extent of damage halos surrounding IR laser pits because analyses cannot be made within the damage zone (Rumble and Hoering, 1994).

3. Ultraviolet laser fluorination

Ablation of biogenic apatite by ultraviolet UV laser in F_2 gas has the potential to eliminate many of the uncertainties that apparently affect accuracy with

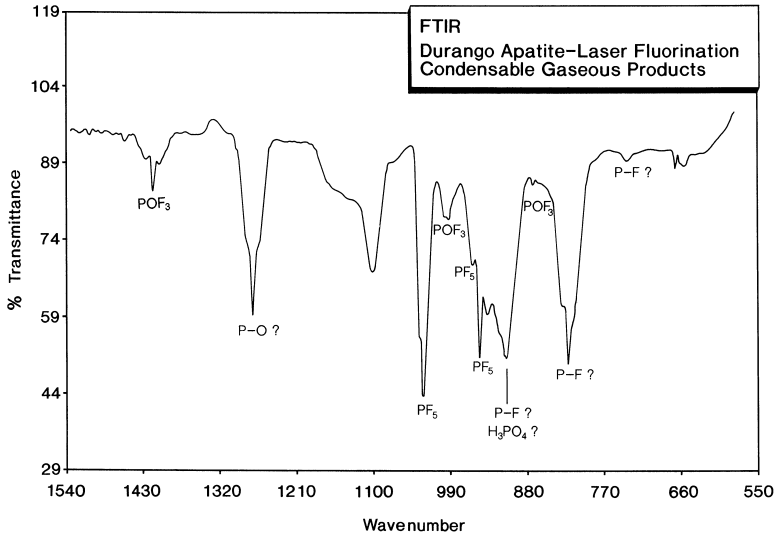

Fig. 2. Infrared absorption spectrum of condensible gases formed during fluorination of fluorapatite by infrared laser heating. Note the presence of PF_5 and POF_3. Bands labelled P–F? may signify the presence of PF_3. Bands near 1280 cm_{-1} are likely P–O bonds resulting from other phosphoryl halides. Band assignments based on data presented by Gutowsky and Liehr (1952), Wilson and Polo (1952) and Downs et al. (1982).

IR laser fluorination of phosphate. UV ablation converts solid phosphate to a plasma thus reducing the opportunity for incomplete breakdown of PO_4^{3-}. Fluorination occurs within the hot plasma where temperatures of 7000–30 000 K (Le et al., 1996) are expected to drive the fluorination reaction to completion, phosphoryl halides are thus not expected to survive the extreme plasma conditions. The efficacy of UV laser fluorination for liberating oxygen in-situ with isotope fidelity from geological samples was demonstrated by Wiechert and Hoefs (1995) and Rumble et al. (1997).

Recently, Young et al. (1998a,b) have shown that UV laser fluorination can be combined with gas chromatography-isotope ratio monitoring mass spectrometry (irm-GCMS) of O_2 gas to reduce the minimum sample size of laser fluorination by a factor of 100.

4. Analytical procedures

UV lasers emit radiation at short wavelengths (e.g., 248 nm, KrF excimer and 255 nm, copper vapour) and the mineral-laser coupling process thus differs from that of the longer wavelength IR laser. When a mineral is irradiated with an IR laser most of the photon energy is converted into vibrational energy within the crystal. The increase in vibrational energy causes heating and finally melting of the irradiated spot. In the case of IR laser heating of phosphate, Cerling and Sharp (1996) state that damage halos around laser pits range from a few hundred to 800 μm in diameter. In contrast, UV laser ablation results in electronic transitions within the material, causing the destruction of chemical bonds with negligible heating of the surrounding mineral (Young et al., 1998b). Sample size is therefore not restricted by the need to overcome melt zone fractionation effects and by using the UV-irms method of Young et al. (1998a), nanomoles of gas can be successfully analysed from 100 μm × 80 μm × 50 μm UV ablation pits, corresponding to ~1 μg of mineral. The lack of reaction rim also allows pits to be continually reablated with no loss of precision.

In this study biogenic apatite samples were analysed by UV laser ablation in F_2 gas using conventional isotope ratio mass spectrometry with the aid of a cold finger 'microvolume' inlet and by irm-GCMS following the method of Young et al. (1998a). PO_4^{3-} data from enamels of varying ages (24.9 ka to 6 Ma) were used for calibration of this method. Ag_3PO_4 analyses were carried out using well established methods (see Iacumin et al., 1996).

4.1. 'Microvolume' analyses

The Oxford laser extraction system has been described previously (Young et al., 1998b). Enamel samples were analysed initially using the cold finger 'microvolume' inlet on the Finnigan MAT 252 gas source mass spectrometer. Successful analyses were performed using 330 mW–500 mW of UV light with a spot size of 25 μm (corresponding to a fluence of 12–18 J/cm^2) and 2–5 mbar of fluorine. Typical sample size was 20 μg, corresponding to ablation pits of 300 μm × 400 μm × 50 μm created by

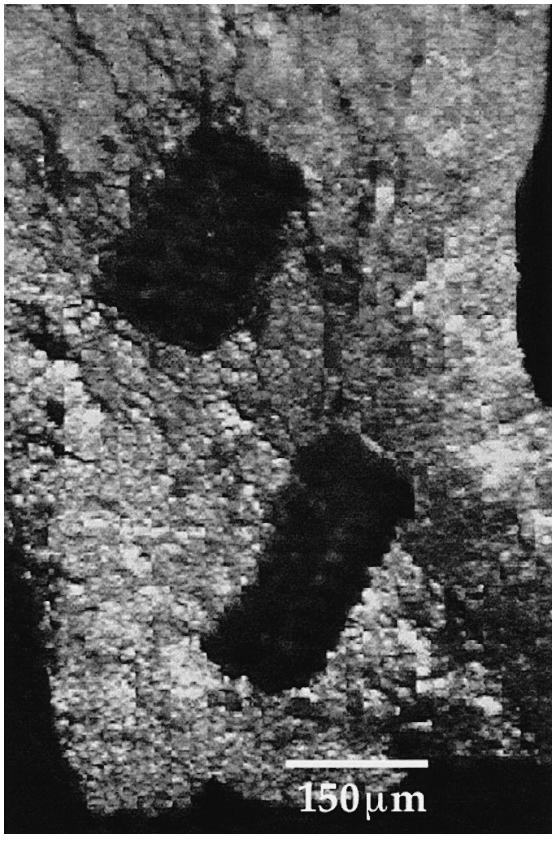

Fig. 3. Photograph showing UV–irm-GCMS laser ablation pits in sample ICT1.

movement of the sample stage beneath the laser beam. Initial mass scans revealed the presence of large amounts of contaminant CF_4 and NF_3, believed to be derived from reaction of F_2 with organics within the enamel. Gold coating of the sample reduced the amount of contaminant fluorides and all experiments were subsequently conducted on gold coated samples. The effect of the gold coating is also beneficial to laser-sample coupling because gold is non-reflective to UV light. All samples were routinely pumped under high vacuum for at least 24 h prior to sample prefluorination to ensure that no atmospheric water was present to form HF or H_3PO_4 upon addition of F_2.

During the course of a day $\delta^{18}O$ values were seen to gradually decay by 1‰ but this slow drift could be successfully avoided by rapid heating of the metal line at 80°C for 20 min between analyses. Blank O_2 was below detection in all 'microvolume' experiments.

Table 1
Comparison of carbonate hydroxylapatite $\delta^{18}O$ and $\delta^{17}O$ values obtained by UV laser fluorination with PO_4^{3-} reference $\delta^{18}O$ values

Specimen	Species	Age	PO_4^{3-} $\delta^{18}O_{VSMOW}$	Microvolume $\delta^{18}O_{VSMOW}$	irm-GCMS $\delta^{18}O_{VSMOW}$	irm-GCMS $\delta^{17}O_{VSMOW}$
ICT1	*Bos primigenius*	Pleistocene	18.0[a]	17.3		
ICT1	*B. primigenius*	Pleistocene		17.3		
ICT1	*B. primigenius*	Pleistocene		17.3		
CT1	*B. primigenius*	Pleistocene		18.1		
ICT1	*B. primigenius*	Pleistocene		18.1		
ICT1	*B. primigenius*	Pleistocene			18.0	9.4
ICT1	*B. primigenius*	Pleistocene			17.9	9.9
ICT1	*B. primigenius*	Pleistocene			17.2	9.4
Mean ($\pm 1\sigma$)				17.6 (0.4)	17.7 (0.4)	9.6 (0.2)
3/1	*Mammuthus primigenius*	Pleistocene	11.4[a]	11.0		
3/1	*M. primigenius*	Pleistocene		10.9		
3/1	*M. primigenius*	Pleistocene		10.8		
3/1	*M. primigenius*	Pleistocene			10.6	6.6
3/1	*M. primigenius*	Pleistocene			10.7	5.0
Mean ($\pm 1\sigma$)				10.9 (0.08)	10.7 (0.05)	5.8 (0.8)
21-5/90-13	*Diceros bicornis*	Recent	20.8[a]	21.3		
21-5/90-13	*D. bicornis*	Recent		21.2		
21-5/90-13	*D. bicornis*	Recent		20.1*		
21-5/90-13	*D. bicornis*	Recent		20.1*		
21-5/90-13	*D. bicornis*	Recent			20.4*	10.4
21-5/90-13	*D. bicornis*	Recent			19.6	10.3
21-5/90-13	*D. bicornis*	Recent			19.7	10.5
21-5/90-13	*D. bicornis*	Recent			20.7	11.0
Mean ($\pm 1\sigma$)				20.6 (0.6)	20.1 (0.4)	10.6 (0.3)
Loth 64e	*Primelephas*[c]	Pliocene	19.9[b]	20.0		
Loth 64e	*Primelephas*	Pliocene		20.0*		
Loth 64e	*Primelephas*	Pliocene		20.0*		
Loth 64e	*Primelephas*	Pliocene		20.8		
Loth 64e	*Primelephas*	Pliocene			21.0	10.7
Loth 64e	*Primelephas*	Pliocene			19.4	10.1
Loth 64e	*Primelephas*	Pliocene			20.3	10.5
Mean ($\pm 1\sigma$)				20.2 (0.3)	20.2(0.6)	10.4(0.3)

* Denotes reablation of a single pit within the sample.
[a] Denotes $\delta^{18}O$ values obtained by Ag_3PO_4 extraction.
[b] Denotes calculated Ag_3PO_4 value from CO_3 data where $\Delta_{PO_4-CO_3} = 9.2‰$ (Iacumin et al., 1996).
[c] Specimen identification difficult owing to fragmentary nature of sample; believed to be either *Primelephas* or *Stegatetrabeledon* (T. Cerling, personal communication).

4.2. Isotope ratio monitoring gas chromatography mass spectrometry

Development of the irm-GCMS system for $^{18}O/^{16}O$ analyses is described in detail by Young et al. (1998a). irm-GCMS allows the transfer of nanomoles of O_2 gas into the mass spectrometer without loss of isotope fidelity thus permitting analysis of pit sizes as small as 80 μm × 80 μm × 50 μm. For most biogenic apatite experiments pit sizes approached 200 μm × 100 μm × 50 μm, corresponding to 3 μg of sample (Fig. 3). Oxygen blanks for irm-GCMS experiments were approximately 1 nmol (generally 1/10 to 1/30 of the sample size) and exhibited stable $\delta^{18}O$ values such that multiple blank analyses were only necessary after loading a new sample into the vacuum system.

5. Results and discussion

All data are shown in Table 1 and Fig. 4 and it is evident that mean laser $\delta^{18}O$ values correspond well to accepted Ag_3PO_4 data. These data show that high resolution analyses can be carried out by UV laser fluorination without data correction factors or the spatial hindrance of laser reaction rims inherent to other laser methods. The $^{17}O/^{18}O$ ratios, generally consistent with mass fractionation, are indicative of the successful separation of oxygen from gaseous fluorides within the GC column.

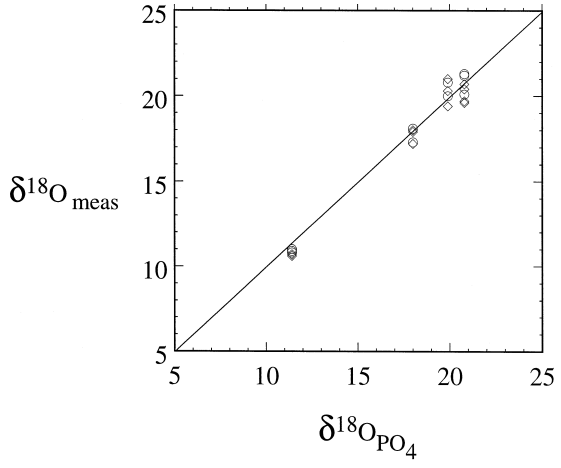

Fig. 4. Enamel $\delta^{18}O$ by UV laser fluorination vs. phosphate $\delta^{18}O$. Circles = 'microvolume', diamonds = irm-GCMS data. The 1:1 line is also shown.

Agreement between laser and Ag_3PO_4 analyses indicates that the hydroxyl and carbonate components compensate for each other isotopically, i.e., $\Delta_{meas-PO_4} \sim 0$ (Fig. 4). Using this information the value of Δ_{OH-PO_4} can be inferred. Based on a typical biogenic apatite, the oxygen contribution from the carbonate group is 7.4%, and from the hydroxyl group it is 4.1%. For $\Delta_{CO_3-PO_4} = 9.2‰$ (Iacumin et al., 1996), Δ_{OH-PO_4} is calculated to be −16.6‰. This value is well within the range of mineral-hydroxyl $^{18}O/^{16}O$ fractionations presented by Zheng (1993).

The laser $\delta^{18}O$ values stay true to Ag_3PO_4 values over a large timescale (24.9 ka to 6 Ma), suggesting that the balance of the carbonate and hydroxyl groups remains constant even in the older specimens. This is an important consideration for all bulk analyses because an unbalanced change in $\delta^{18}O$ values or amount of carbonate and hydroxyl could result in unreliable $\delta^{18}O$ data.

$\delta^{18}O$ Variations in some specimens may indeed be real variations corresponding to changes in the animal's drinking water intake. Such variations have been noted in previous studies (Fricke and O'Neil, 1996; Bryant et al., 1996a,b; Stuart-Williams et al., 1997; Fricke et al., 1998a,b; Sharp and Cerling, 1998) where spatial resolution on the mm scale is sufficient for resolving subannual variability. The higher resolution of the UV laser method will allow such studies to be extended to analyses at monthly or submonthly intervals. This study has not, however, specifically addressed along tooth variations.

Using the UV laser, analyses can be made adjacent to one another because no damage surrounds UV laser pits. The minimum analysis spot dimension of ~80 μm is dictated by the 1 nmol oxygen blank; smaller craters require larger blank correction. Reduction in blank would, however, permit spatial resolution of ~40 μm from spot to spot (Young et al., 1998a). UV laser pits can also be reablated with no loss of precision (see Table 1) providing a means of obtaining high resolution 3-D $\delta^{18}O$ data. $\delta^{18}O$ changes with tooth growth could potentially be monitored in this way.

6. Conclusions

This study has shown that $^{18}O/^{16}O$ of biogenic phosphates can be determined by UV laser fluorination with a combination of spatial (~ 100 μm) and analytical (± 0.4‰, 1σ) resolution unobtainable by chemical extraction or IR laser methods. Intratooth $\delta^{18}O$ analyses at this scale have the potential to supply palaeoclimatological information at monthly, or submonthly, intervals.

The data also indicate that the isotopic compositions of hydroxyl and carbonate components tend to compensate one another and thus have little effect on bulk hydroxylapatite $\delta^{18}O$ values. Studies will be necessary to investigate this relationship further into the geological past where diagenetic effects may play a greater role.

Acknowledgements

The spectroscopic study was performed while one of the authors (E.D.Y.) was a postdoctoral fellow at the Carnegie Institution of Washington's Geophysical Laboratory. Dr. Thomas Hoering (deceased) and Dr. Bjorn Mysen are gratefully acknowledged for their invaluable help in obtaining the spectroscopy data presented here. A.M.J. also thanks Henry Fricke and Marilyn Fogel, for useful discussions, and Douglas Rumble (III), for hospitality, while at the Geophysical Laboratory. Thanks also to Paul Koch for advice and donation of Sample 21-5/90-13 and to T. Cerling for Sample Loth 64e. L.K. Ayliffe and Henry Fricke are thanked for their constructive reviews. Nicholas Gardiner is acknowledged for his contribution to initial development of the Oxford laser fluorination line. This work was supported by a NERC studentship grant to A.M.J.

References

Ayliffe, L.K., Chivas, A.R., 1990. Oxygen isotope composition of the bone phosphate of Australian kangaroos: potential as a paleoenvironmental recorder. Geochimica Cosmochimica Acta 54, 2603–2609.

Ayliffe, L.K., Chivas, A.R., Leakey, M.G., 1994. The retention of primary oxygen isotope compositions of fossil elephant skeletal phosphate. Geochimica Cosmochimica Acta 58, 5291–5298.

Bryant, J.D., Froelich, P.N., Showers, W.J., Genna, B.J., 1996a. A tale of two quarries: biologic and taphonomic signatures on the oxygen isotope composition of tooth enamel phosphate from modern and Miocene equids. Palaios 11, 397–408.

Bryant, J.D., Froelich, P.N., Showers, W.J., Genna, B.J., 1996b. Biologic and climatic signals in the oxygen isotopic composition of Eocene–Oligocene equid enamel phosphate. Palaeogeography, Palaeoclimatology, Palaeoecology 126, 75–89.

Cerling, T.E., Sharp, Z.D., 1996. Stable carbon and oxygen isotope analysis of fossil tooth enamel using laser ablation. Palaeogeography, Palaeoclimatology, Palaeoecology 126, 173–186.

D'Angela, D., Longinelli, A., 1990. Oxygen isotopes in living mammal's bone phosphate: further results. Chemical Geology 86, 75–82.

Downs, A.J., Gaskill, G.P., Saville, S.B., 1982. Oxygen atom transfer in low-temperature matrices: 1. Formation and characterization of matrix-isolated OMF_3 (M = P, As)[1a]. Inorganic Chemistry 21, 3385–3393.

Fricke, H.C., O'Neil, J.R., 1996. Inter- and intra-tooth variations in the oxygen isotope composition of mammalian tooth enamel phosphate: implications for palaeoclimatological and palaeobiological research. Palaeogeoraphy, Palaeoclimatology, Palaeoecology 126, 91–99.

Fricke, H.C., Clyde, W.C., O'Neil, J.R., 1998a. Intra-tooth variations in $\delta^{18}O$ (PO_4) of mammalian tooth enamel as a record of seasonal variations in continental climate variables. Geochimica Cosmochimica Acta 62, 1839–1851.

Fricke, H.C., Clyde, W.C., O'Neil, J.R., Gingerich, P.D., 1998b. Evidence for rapid climate change in North America during the latest Paleocene Thermal Maximum: oxygen isotope compositions of biogenic phosphate from the Bighorn Basin (Wyo.). Earth and Planetary Science Letters 160, 193–209.

Gutowsky, H.S., Liehr, A.D., 1952. The infrared spectra of PF_3, POF_3, and PF_5. Journal of Chemical Physics 20, 1652–1653.

Iacumin, P., Bocherens, H., Mariotti, A., Longinelli, A., 1996. Oxygen isotope analyses of co-existing carbonate and phosphate in biogenic apatite: a way to monitor diagenetic alteration of bone phosphate. Earth and Planetary Science Letters 142, 1–2.

Kohn, M.J., Schoeninger, M.J., Valley, J.W., 1996. Herbivore tooth oxygen isotope compositions: effects of diet and physiology. Geochimica Cosmochimica Acta 60, 3889–3896.

Kolodny, Y., Luz, B., Navon, O., 1983. Oxygen isotope variations in phosphate of biogenic apatites: I. Fish bone apatite—rechecking the rules of the game. Earth and Planetary Science Letters 64, 398–404.

Le, H.C., Vuillon, J., Zeitoun, D., Marine, W., Sentis, M., Dreyfus, R.W., 1996. 2D modelling of laser-induced plume expansion near the plasma ignition threshold. Applications of Surface Science 96–98, 76–91.

Longinelli, A., 1984. Oxygen isotopes in mammal bone phosphate: a new tool for paleohydrological and paleoclimatological research?. Geochimica Cosmochimica Acta 48, 385–390.

Luz, B., Kolodny, Y., Kovach, J., 1984. Oxygen isotope varia-

tions in phosphates of biogenic apatites: III. Conodonts. Earth and Planetary Science Letters 69, 255–262.

Luz, B., Kolodny, Y., 1985. Oxygen isotope variations in phosphate of biogenic apatites: IV. Mammal teeth and bones. Earth and Planetary Science Letters 75, 29–36.

McConnell, D., 1973. Apatite—Its Crystal Chemistry, Mineralogy, Utilization and Geologic and Biologic Occurrences. Springer-Verlag.

O'Neil, J.R., Roe, L.J., Reinhard, E., Blake, R.E., 1994. A rapid and precise method of oxygen isotope analysis of biogenic phosphate. Israeli Journal of Earth Sciences 43, 203–212.

Rumble, D. III, Hoering, T.C., 1994. Analysis of oxygen and sulfur isotope ratios in oxide and sulfide minerals by spot heating with a carbon dioxide laser in a fluorine atmosphere. Accounts of Chemical Research 27, 237–241.

Rumble, D. III, Farquhar, J., Young, E.D., Christensen, C.P., 1997. In situ oxygen isotope analysis with an excimer laser using F_2 and BrF_5 reagents and O_2 gas as analyte. Geochimica Cosmochimica Acta 61, 4229–4234.

Sharp, Z.D., Cerling, T.E., 1996. A laser GC-IRMS technique for in situ stable isotope analyses of carbonates and phosphates. Geochimica Cosmochimica Acta 60, 2909–2916.

Sharp, Z.D., Cerling, T.E., 1998. Fossil isotope records of seasonal climate and ecology: straight from the horse's mouth. Geology 26, 219–222.

Stuart-Williams, H., Le, Q., Schwarcz, H.P., 1995. Oxygen isotopic analysis of silver orthophosphate using a reaction with bromine. Geochimica Cosmochimica Acta 59, 3837–3841.

Stuart-Williams, H., Le, Q., Schwarcz, H.P., 1997. Oxygen isotopic determination of climatic variation using phosphate from beaver bone, tooth enamel and dentine. Geochimica Cosmochimica Acta 61, 2539–2550.

Wiechert, U., Hoefs, J., 1995. An excimer laser-based microanalytical preparation technique for in situ oxygen isotope analysis of silicate and oxides minerals. Geochimica Cosmochimica Acta 59, 4093–4104.

Wilson, M.K., Polo, S.R., 1952. The infrared spectra of NF_3 and PF_3. Journal of Chemical Physics 20, 1716–1719.

Wright, E.K., Hoering, T.C., 1989. Separation and purification of phosphates for oxygen isotope analysis. Annual Report of the Geophysical Laboratory, Carnegie Institute, Washington DC 1988–1989, Vol. 2150, pp. 137-141.

Young, E.D., 1993. Oxygen isotope ratio analysis of phosphate in biogenic and non-biogenic apatite by laser heating in F_2 gas: a spectroscopic study of the fluorination process. Geological Society of America Abstracts Program 25, A205.

Young, E.D., Fogel, M.L., Rumble III, D., Hoering, T.C., 1998a. Isotope-ratio-monitoring of O_2 for microanalysis of $^{18}O/^{16}O$ and $^{17}O/^{16}O$ in geological materials. Geochimica Cosmochimica Acta, in review.

Young, E.D., Coutts, D.W., Kapitan, D., 1998b. UV laser ablation and irm-GCMS microanalysis of $^{18}O/^{16}O$ and $^{17}O/^{16}O$ with application to a calcium–aluminium-rich inclusion from the Allende meteorite. Geochimica Cosmochimica Acta, in review.

Zheng, Y.-F., 1993. Calculation of oxygen isotope fractionation in hydroxyl-bearing silicates. Earth and Planetary Science Letters 120, 247–263.